Engineering Transactions, **67**(1): 133–142, 2019, doi: 10.24423/EngTrans.944.20190214
Polish Academy of Sciences • Institute of Fundamental Technological Research (IPPT PAN)
Université de Lorraine • Poznan University of Technology

ICPS5

Experimental and Analytical Investigation of Point Fixed Corrugated Metal Sheets Subjected to Blast Loading

Kai FISCHER*, Alexander STOLZ, Christoph ROLLER

[1)] *Fraunhofer Institute for High-Speed Dynamics, Ernst-Mach-Institut*
Efringen-Kirchen, Germany
*Corresponding Author e-mail: kai.fischer@emi.fraunhofer.de

Besides the primary threats of a blast loading scenario, flying fragments from non-structural elements could be a further threat to exposed humans. Point fixed corrugated metal sheets are often applied as facade elements. This paper focuses on the analysis of the dynamic bearing resistance and related pull-out behaviour of such elements.

In a first step, the dynamic bearing capacity is investigated by an experimental study. Different sheet thicknesses and dimensions are examined for different loading levels using shock tube experiments. Based on the experimental results an engineering model is applied to predict the overall bearing capacity of the investigated corrugated metal sheet elements using mathematical optimisation methods.

In a second step, the comparison to an analytical approach to quantify the prognostic capacity of the theoretical assessment method is addressed. Obtained results enable fast and effective quantification of expected damage effects and can be integrated into an overall risk and resilience analysis scheme.

Key words: SDOF modelling; shock tube testing; corrugated metal sheets; blast loading.

1. Introduction

Effective and systematic risk management methodologies are essential to evaluate critical infrastructure elements or industrial plants [1]. To identify a desired level of safety, it is essential to identify potential hazards and the resulting expected damage effects in case of event occurrence. The results will identify structural deficits for the excepted loading behaviour or evaluate the effectiveness of enhancement measures.

Explosion events, such as accidents on an industrial site or a terrorist event, cause different hazard sources. Besides primary hazards, such as the shock wave, secondary hazards such as flying fragments can threaten exposed humans in the surrounding of the hazard source. The damage of the power plant after the Evangelos Florakis Naval Base explosion in 2011 is an example where the pull

out of several façade elements designed with cold-formed corrugated metal sheets caused serious harm to exposed individuals.

For an adequate risk analysis considering these loading cases knowing the effects of the loading on the point fixed corrugated metal is essential. Hence, the response behaviour of point fixed corrugated metal sheets has to be analysed to obtain information concerning the hazard potential to exposed humans. In general, position stability, i.e., the plate is plastically damaged but still in place, is required as a sufficient safety level.

Numerical or experimental investigations are possible/feasible, realisable but expensive in costs and time, especially when the configuration or the hazard scenario changes. A generalised engineering model with a focus on the failure behaviour is available [2] and its accuracy will be compared using a shock tube test series. This paper focusses on the comparison of an engineering model with an experimental test series to evaluate the accuracy of that model. In a first step, the test setup and the results are presented. Afterwards, the model and the comparison to the experiments are discussed.

2. Experimental investigations

The structural analysis of point fixed trapezoidal sheets under blast loading is investigated within an experimental test series. The aim of this investigation is the identification of failure mechanisms and the limit of the load-bearing capacity.

The dynamic experimental investigation is performed at the shock tube facility, which simulates a reproducible shock wave with compressed air. A generalised sketch/schematic of the facility is shown in Fig. 1. Air is compressed within a pressure chamber, which is separated from the residual facility by a membrane. If a required filling pressure is achieved, a mechanical device opens the membrane, and the compressed air propagates within the expansion section. A plane shock wave arises within the transition and impinges on the fixed structural member at the end of the tube. In contrast to free field experiments, shock tube

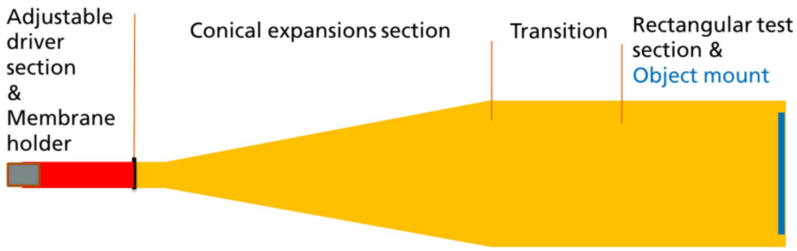

Fig. 1. Sketch and identification of single areas of the shock tube facility.

tests have a better reproducibility, excluding clearing effects, and deviations are smaller.

The rectangular test section has a maximum dimension of 3 by 3 m and an adjustable frame for structural members with smaller dimensions. Figure 2 shows the setup to examine the structural response of the sheet metal, which has a length of 2.8 m and a width of 1.04 m. The structural member is fixed at every profile bottom onto a steel bar in the frame of the shock tube to increase the resistance against direct shearing failure at the screw connection. The picture on the right in Fig. 2 shows the result after a test with a higher loading level.

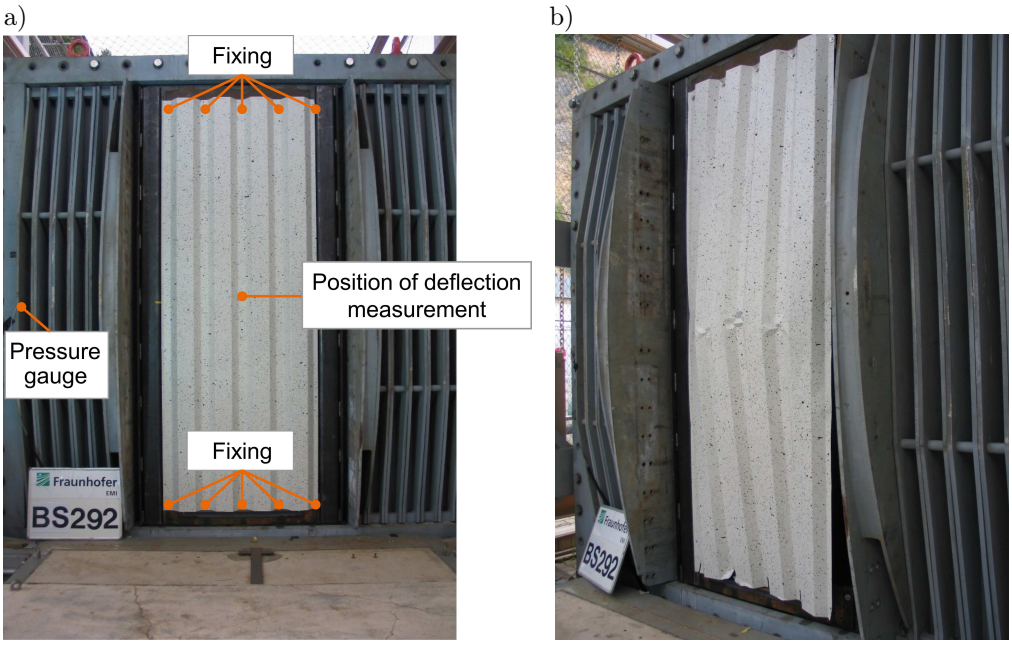

FIG. 2. Experimental setup at the shock tube facility to analyse the dynamic behaviour of point fixed trapezoidal sheets (a) and the structural response after the test with the failure at the screw connections (b).

A displacement gauge measures the deflection-time relationship during a test, and pressure gauges inside the facility measure the pressure-time history of the simulated shock wave. A high-speed camera is applied to gather detailed optical information of the dynamic behaviour.

In summary, 30 tests were carried out for different loading levels and two different plate thicknesses. Figure 3 compares the deflection-time relationships of the test series, which were measured at the middle of the fixed test device. The two pictures on the right side show the response at the fixing after the test. With the lowest loading level (5 kPa overpressure, green curve) an elastic

response is observed, and the structural member bends back in the unloaded starting position. The black curves (10 kPa overpressure) indicate the response with slight yielding at the fixing, as shown in the lower picture on the right side of Fig. 3 at a screw connection. These tests result in a larger maximum deflection, the connections just withstand the load, and the structure bends back to zero. The highest loading level (15 kPa overpressure) results in single failure at the support, see the upper picture on the right side of Fig. 3 where single screws are breached out and the measured deflection is shown with the red curves, the structure results in yielding, and behaviour with no further oscillation of the investigated sheet is observed.

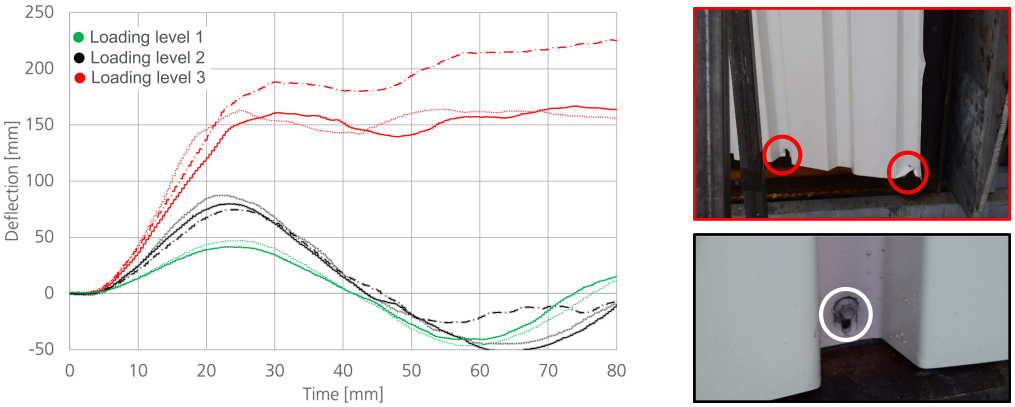

FIG. 3. Comparison of the measured deflection-time histories during the dynamic tests. The pictures indicate the structural response with slight yielding of the sheet at the fixing (lower picture) and a single failure of the sheet at the support (upper picture). The investigated failure at the support is marked with circles in the pictures.

In summary, the following findings are observed from the shock test series:

- The investigated structural member fails mainly at the support of the setup. A critical yielding of the metal sheet or shearing of the screw itself is not observed.
- The main failure criterion is based on bearing stress or shear resistance at the support, and smaller proportions are attributed to the buttoning-through of the screws, which will stipulate the bearing failure at the support.

The dynamic tests at the shock tube produced mainly a failure behaviour at the fixing of the sheet. An increased load resulted in larger deflections in the middle of the structure and hence an increasing support rotation between the bending line and the unstressed start configuration.

3. Analytical dynamic bearing model

In addition to experimental investigations and numerical finite-element simulations, fast running engineering models are common practice for structural verification [3]. The bending behaviour and failure of a structural member under dynamic loading are often modelled with a single degree of freedom model (SDOF) [4–6]. With the SDOF model, the structural element is idealised in a single mass point, and the horizontal movement is considered to evaluate the response behaviour as observed with the experimental investigations in the diagram of Fig. 3. The idealisation of the structural element can be expressed by adynamic force equilibrium, see Eq. (3.1)

$$
\begin{aligned}
k_M \cdot m \cdot \ddot{x} &= k_L \left(A \cdot p(t) - R(x) \right), \\
p(t) &= p_{ro} \left(1 - \frac{t}{t_+} \right), \\
R(x) &= A \cdot \frac{2p_0}{\pi} \arctan \left(\frac{\pi c_0 x}{2p_0} \right).
\end{aligned}
\tag{3.1}
$$

In Eq. $(3.1)_1$, the deflection and the acceleration of the mass are expressed by x and respectively $\ddot{x}$. As observed in the dynamic tests (Fig. 3), the maximum deflection arises at the first peak, and it should be noted that the effect of damping on the first peak is normally negligible. Therefore, a viscous damping term is neglected in the range of a transient loading situation [7].

The external force is considered as the product of the surface of the structural element and the pressure-time relationship of the dynamic loading $F(t) = A{\cdot}p(t)$. The pulse loading $p(t)$ is idealised expressed as a linear function depending on the peak overpressure p_{ro} and the duration of the positive overpressure t_+.

To transform the structural element of into an equivalent mass-spring model, the mass and loading factors (k_L, k_M) have to be introduced to represent the equivalent kinetic and strain energy in the model [5]. These factors are derived from deflected shape functions to ensure an equivalent deflection of the mass point in comparison to the real structural member. Dimension and material properties define the resistance of the structural member, and this behaviour is expressed by $R(x)$ in Eq. (3.1). The accuracy of an SDOF model depends on the choice of an adequate deflection-dependent resistance function. A typical resistance shape for ductile bending elements is an arctangent formulation as shown in Eq. (3.1). This functional resistance shape is often applied to evaluate wall elements due to blast loading [8, 9]. In this formulation, p_0 describes the asymptotic response pressure and c_0 the stiffness of the material. The dimensions of the structural member have a significant influence on the resistance behaviour. A thicker structural member results in an increasing p_0 value and a stiffer system

or an increasing length of the structure causes a softer system (decreasing c_0 and p_0), for example.

The inverse approach of [10] results in a direct and dynamic determination of resistance parameter by the comparison between the SDOF model solution and the measured deflection-time history from shock tube tests. By variation of the stiffness (c_0) and the response pressure (p_0) the solution of Eq. (3.1) is optimised by a least-square fit. The inverse approach of [10] results in the qualitatively best resistance parameter considering the dynamic characteristic, such as the strain rate effects, but the solution is only valid for the investigated setup and structural dimensions. If divergent dimensions or material properties are considered, the inverse approach has to be applied to a new experimental test series.

Analytical derivations are a further option to determine the required resistance parameter of the SDOF model. In this study, the approach of [11] is applied and a comparison to the inverse approach [10] evaluates the quality of the analytical approach. Figure 4 shows a sketch of the idealised resistance shape according to the analytical approach [11] in comparison to the real behaviour. In alignment to the resistance function in Eq. (3.1), the response pressure is equal to the ultimate resistance r_u in Fig. 4, and the stiffness is derived with the ultimate resistance in relation to the elastic limit x_E

$$c_0 = \frac{p_0}{x_E}, \qquad p_0 = r_u. \tag{3.2}$$

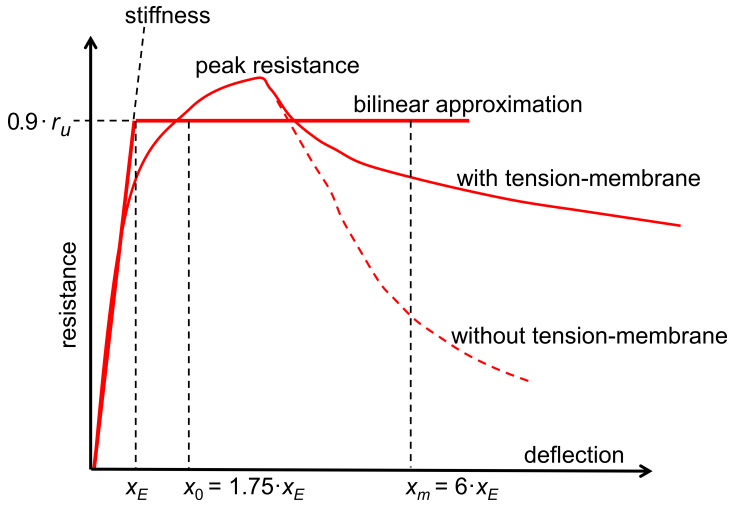

FIG. 4. Sketched resistance behavior of cold-formed steel (thin line) and the idealised bilinear characterisation (thick line) according to [11]. A differentiation of tension-membrane forces characterises the yielding of the material.

Within the calculation of [11], the dynamic yield strength f_{dy} is derived with the static value f_y multiplied with a dynamic increase factor and an average strength factor. Assuming validity of Bernoulli's hypothesis, this quantity and the section modulus W deliver the maximum moment

$$M_R = f_{dy} \cdot W,$$
$$W = \frac{I_{\text{eff}}}{z_{\max}}. \tag{3.3}$$

The quantity derived in Eq. (3.3) in relation to the length of the structure quantifies the ultimate resistance, i.e., the maximum response pressure. The real course of the resistance behaviour is non-linear, as shown in Fig. 4. With the bilinear approximation according to [11], a safety coefficient of 0.9 is considered

$$r_u = 0.9 \cdot \frac{8 \cdot M_R}{L^2}. \tag{3.4}$$

Finally, the elastic limit is quantified with the ultimate resistance r_u, the length L, Young's modulus E, the moment of inertia I_{eff}, and the coefficient γ, which depends on the edge conditions of the system

$$x_E = \frac{\gamma \cdot r_u \cdot L^4}{E \cdot I_{\text{eff}}}. \tag{3.5}$$

The analytical approach, according to Eqs (3.3)–(3.5), is applied to the considered experimental setup and the comparison to the inverse approach shows a good agreement concerning the derived stiffness. Due to the level of simplification and neglect of slipping effects, as expected, both numerical models predict in general a stiffer component response than observed in the experiment. The comparison of the inverse or dynamic response pressure shows a stronger deviation, where the analytical approach results in smaller quantities. This result is also observed in the comparison to experimental tests with nonlinear behaviour of the material, see the red graphs in Fig. 5. The analytical model overestimates the maximum deflection with approximately 20%. Based on these findings, it is proposed to apply the SDOF model of Eq. (3.1) with an adapted response pressure, based on the ultimate analytical resistance of Eq. (3.4)

$$p_0 = 3 \cdot r_u. \tag{3.6}$$

The adapted model with the use of Eq. (3.6) is compared with all tests in a pressure-impulse diagram, see Fig. 6. The colour code indicates the structural

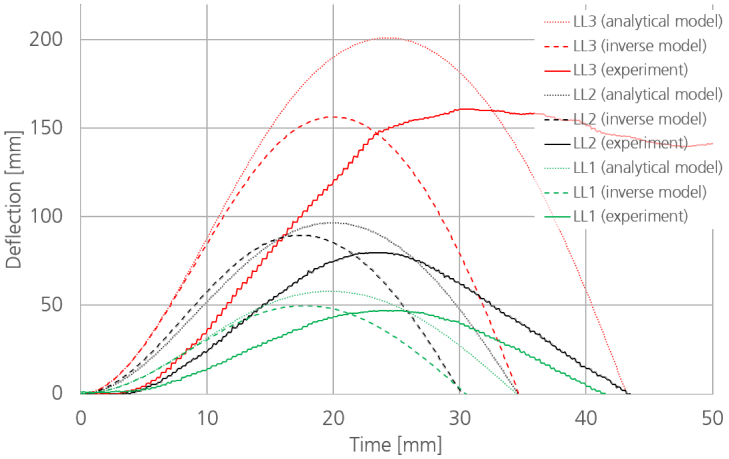

FIG. 5. Comparison of the experimental deflection, the dynamic derived model and the analytical model. The acronym "LL" indicates the corresponding loading level. The analytical model neglects the characteristics of the fixing.

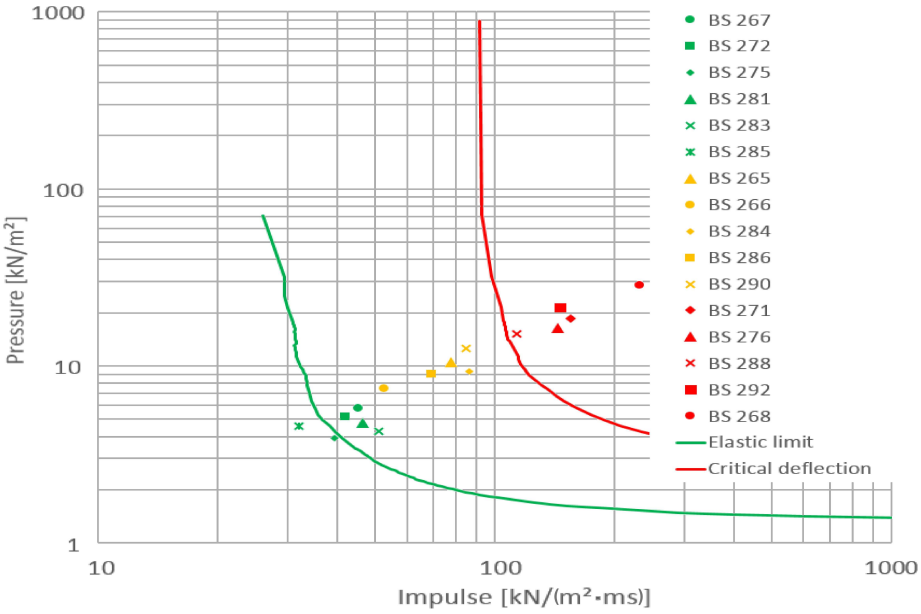

FIG. 6. Comparison of the adapted dynamic model with obtained pressure and impulse values of the test series.

response with elastic behaviour (green), plasticisation (yellow) and failure (red). The green curve indicates the iso-damage curve for the elastic limit and the red curve model failure. Finally, the adapted model indicates similar predictions to the experimental results.

4. Summary

The evaluation of structural elements subjected to blast loading can be assessed with the use of simplified engineering models. Single degree of freedom models provide the basis to derive iso-damage curves within a pressure-impulse diagram to assess the overall response behaviour.

In this paper, the resistance behaviour of point-fixed corrugated metal sheets is analysed. Within an experimental shock tube test series, the failure behaviour is investigated and deflection and pressure time histories are collected for the comparison with the engineering models.

The obtained information is applied to optimise a single degree of freedom model. An analytical model is applied to characterise the bending behaviour of the structural member.

The optimised model is applied within a pressure-impulse diagram and shows sufficient accuracy. Finally, this model can be applied for arbitrary metal sheet configurations and provides contributions within a systematic risk management procedure.

References

1. Assael M.J., Kakosimus K.E., *Fires, explosions, and toxic gas dispersions. Effects calculation and risk analysis*, CRC Press, Boca Raton, 2010.

2. U.S. Army Corps of Engineers, *UFC 3-340-02: Structures to resist the effects of accidental explosions*, U.S. Department of Defense, Washington D.C., USA, 2008.

3. Riedel W., Fischer K., Kranzer C., Erskine J., Cleave R., Hadden D., Romani M., *Modeling and validation of a wall-window retrofit system under blast loading*, Engineering Structures, **37**: 235–245, 2012.

4. Morison C.M., *Dynamic response of walls and slabs by single-degree-of-freedom analysis – a critical review and revision*, International Journal of Impact Engineering, **32**(8): 1214–1247, 2006.

5. Krauthammer T., *Modern protective structures*, CRC Press, Boca Raton, 2008.

6. Mays G.C., Smith P.D., *Blast effects on buildings: Design of buildings to optimize resistance to blast loading*, Thomas Telford Ltd, London, 2009.

7. Biggs J., *Introduction to structural dynamics*, McGraw-Hill Book Company, New York, 1964.

8. Mayrhofer C., *Reinforced masonry walls under blast loading*, International Journal of Mechanical Sciences, **44**(6): 1067–1080, 2002.

9. Stolz A., Fischer K. Roller C., Hauser S., *Dynamic bearing capacity of ductile concrete plates under blast loading*, International Journal of Impact Engineering, **69**: 25–38, 2014.

10. Fischer K., Häring I., *SDOF response model parameters from dynamic blast loading experiments*, Engineering Structures, **31**(8): 1677–1686, 2009.

11. U.S. Army Corps of Engineers, *UFC 3-340-02: Structures to resist the effects of accidental explosions*, Departments of the Army, the Navy, and the Air Force, 2008.

Received July 23, 2018; accepted version September 22, 2018.
